PNAS RESEARCH ARTICLE | NEUROSCIENCE

A circuit model for transsaccadic space updating and mislocalization

Xiao Wang[a,b], Sophia J. Tsien[c], Min Jin[a], Michael E. Goldberg[d,e,f,g,1], Mingsha Zhang[a,1], and Ning Qian[d,h,1]

Affiliations are included on p. 9.

Contributed by Michael E. Goldberg; received November 4, 2024; accepted April 3, 2025; reviewed by David C. Burr and Marc A. Sommer

We perceive a stable, continuous world despite drastic changes of retinal images across saccades. However, while *persistent* objects in daily life appear stable across saccades, stimuli *flashed* around saccades can be grossly mislocalized. We address this puzzle with our recently proposed circuit model for perisaccadic receptive-field (RF) remapping in the lateral interparietal area (LIP) and frontal eye fields (FEF). The model uses center-excitation/surround-inhibition connections to store a relevant stimulus' retinal location in memory as a population activity. This activity profile is updated across each saccade by directional connections gated by the corollary discharge (CD) of the saccade command. The updating is a continuous backward (against the saccade) shift of the population activity (equivalent to continuous forward remapping of the RFs), whose cumulative effect across the saccade is a subtraction of the saccade vector. The model that correctly updates persistent stimuli, and flashes well before and after saccades, produces the observed forward and backward translational mislocalization for flashes around the saccade onset and offset, respectively, because of insufficient and unnecessary cumulative updating after the saccade, caused by visual response latency and sluggish CD time course. We confirm the model prediction that for perisaccadic RFs measured with flashes before the saccades, the forward remapping magnitudes across the saccades are smaller for later flashes. Our work suggests that transsaccadic perception is stable because the presaccadic retinal position of an object is updated to match the postsaccadic (reafferent) retinal position of the same object, and that the brain uses "unaware" decoders which do not distinguish between different origins of neurons' activities.

RF remapping | aware and unaware decoders | memory mislocalization | efference copy | double-step saccade

Significance

Transsaccadic space perception is a central topic of visuomotor research. Many studies have been devoted to this topic, yet there is little coherence among them. For example, receptive-field (RF) remapping is considered a physiological substrate for stable space perception across saccades, but is also believed to cause perisaccadic mislocalization, a form of perceptual instability. Here, we propose a simple computational mechanism that integrates the physiological properties of RF remapping, the functional requirement of stable space perception across saccades, and the psychophysical observations of perisaccadic mislocalization. Our work also suggests that the brain's positional decoders interpret a cell's response in the same way regardless of whether the response is from the stimulation of the cell's RF or remapped laterally from elsewhere.

We make several saccades per second to look at different parts of a scene for high-resolution processing. Across a saccade the retinal image changes drastically, yet the world appears stable and continuous to us. Two main mechanisms have been proposed to explain this phenomenon of transsaccadic visual stability (TSVS): i) the brain combines eye-position signals and retinotopic inputs to construct craniotopic (head-centered) representations (1–4), and ii) the brain uses corollary discharges (CDs) of saccade commands to "compensate" for saccade-induced retinal changes (5–8). These mechanisms appear to contribute to transsaccadic space perception at long- and short-time scales, respectively (9, 10). Here, we focus on the CD mechanism because we would like to link its detailed, transsaccadic operations to the short-time-scale phenomenon of perisaccadic perceptual mislocalization. We consider saccades under the head-fixed condition so that the display screen for stimuli is craniotopic.

The original proposal of the CD mechanism is that the CD of a saccade cancels the retinal image motion produced by the saccade (5). A related observation is saccadic suppression: During saccades, visual perception (particularly of magnocellular stimuli such as motion) is impaired (11), and correspondingly, some visual neurons have reduced responses or reversed directional tuning (12, 13). There is evidence that CDs contribute to saccadic suppression (12), although less than forward and backward masking (14). However, while cancellation and/or suppression of saccade-induced retinal motion may contribute to TSVS, they are insufficient. Consider the double-step memory saccade task, a standard demonstration of TSVS, in which subjects sequentially make saccades to two successively flashed and disappeared targets (Fig. 1). In a craniotopic representation, the position of the second target (diamond) does not change with the first saccade (the rightward black arrow, Fig. 1*A*). However, in a retinotopic representation, since the first saccade changes the retinal position of the second target (from the magenta to green arrow), the brain must update the retinal position of the second target, by subtracting the saccade vector, before making the second saccade (Fig. 1*B*). Canceling or suppressing the

Author contributions: S.J.T., M.E.G., M.Z., and N.Q. designed research; X.W. and S.J.T. performed research; X.W. and M.J. analyzed data; and X.W., M.E.G., M.Z., and N.Q. wrote the paper.

Reviewers: D.C.B., Universita degli Studi di Firenze; and M.A.S., Duke University.

The authors declare no competing interest.

[1]To whom correspondence may be addressed. Email: meg2008@columbia.edu, mingsha.zhang@bnu.edu.cn, or nq6@columbia.edu.

This article contains supporting information online at https://www.pnas.org/lookup/suppl/doi:10.1073/pnas.2422911122/-/DCSupplemental.

Published May 19, 2025.

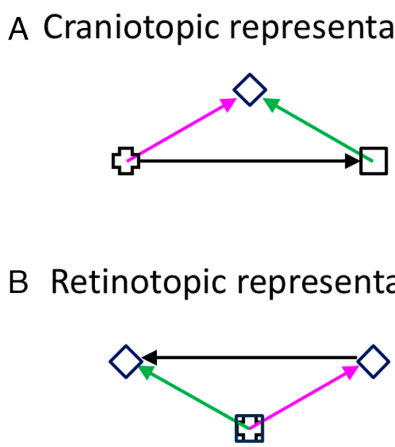

Fig. 1. Double-step memory saccade task: the updating of the second target across the first saccade. (*A*) Craniotopic (screen) representation. After subjects fixate on the cross, the cross disappears, and the square and diamond are flashed successively. Subjects then sequentially saccade to the remembered square and diamond positions. (*B*) Retinotopic representation across the first saccade (back projected from the retina to the screen for comparison with *A*). The cross and square are superimposed as they correspond to the same retinal position, the fovea. The magenta and green arrows indicate the diamond's retinotopic positions before and after the first saccade (the rightward black arrow in *A*), respectively. The leftward black arrow indicates that the diamond's retinotopic position needs to be updated backward by subtracting the saccade vector.

saccade-induced retinal motion would not provide the required updating. Moreover, the two saccades of this task can be made in total darkness; in this case there is no retinal motion to cancel or suppress but to make the second saccade, the brain still must update the retinal location of the second target.

The discovery of the CD-driven receptive-field (RF) remapping in LIP and FEF (6–8, 15–17) has inspired new proposals on how the CD mechanism enables TSVS. The remapping refers to the observation that around the time of a saccade, cells' RFs (perisaccadic RFs or pRFs) shift in the saccade (forward) direction. Early remapping studies focused on the fact that some cells show visual responses at their future (postsaccadic) RF (fRF) locations, accompanied by reduced responses at the current (presaccadic) RF (cRF) locations, even before the saccade onset. [A cell's cRF and fRF are just its ordinary RF well before and well after the saccade, respectively; for a retinotopic cell, its cRF and fRF are offset by the saccade size on the display screen but superimpose on the retina. We use their screen (craniotopic) positions unless noted otherwise]. This leads to the Preview Theory of TSVS (6, 18): On the screen, a cell's fRF before a saccade will become its actual RF after the saccade. The activation of a cell by a stimulus in its fRF can thus be considered as giving the cell a preview of what will be in its RF after the saccade. Then, a comparison between the preview response and the postsaccadic (reafferent) response can determine whether the stimulus is the same or different across the saccade.

Although intuitively appealing, the Preview Theory has a few difficulties. First, it requires cells whose pRFs remap completely to their fRFs without responses at their cRFs (or any other positions) before saccades. Otherwise, the preview responses would represent a mixture of stimuli in both the cRFs and fRFs, complicating the postsaccadic comparison. Second, the theory requires downstream stages that store the preview responses in memory and then compare them with the postsaccadic responses later. These memory and comparison stages have not been identified (19). Finally, for the double-step memory saccade task mentioned above, the flashed targets disappear before the first saccade, and they do not reappear to generate postsaccadic responses for comparison with the preview responses.

Later remapping studies revealed the details of the remapping time course in LIP and FEF (8, 16). Although some cells respond to stimuli in their fRFs before the saccades, on average cells' pRFs shift progressively from their cRF locations to near their fRF locations over time, from about 100 ms before the saccade to about 100 ms after the saccade. (The pRFs were measured with dots flashed *before* the saccade onset.) The pRFs thus move through intermediate locations instead of jumping from the cRFs to the fRFs directly, posing further difficulties for the Preview Theory. There is, however, an alternative solution for TSVS which focuses on the stimulus location, not its features/contents (8). First note that the perceived location of a given stimulus must be decoded from the responses of many cells with different RF locations (population response), instead of from any individual cell's responses to different stimulus locations (spatial tuning or RF) (20). The population response profile is the cells' responses to the stimulus as a function of their RF center locations. When the RFs remap, positional decoders may consider the population response as a function of either the cells' remapped RF locations or the original RF locations; we denote decoders with these alternatives as "aware" and "unaware" decoders, respectively (20). Unaware decoders always interpret cells' responses as evidence for a stimulus in their cRFs regardless of whether the responses indeed originate from their cRFs or are remapped from elsewhere (*Discussion*). Under the assumption of unaware decoders, the progressive *forward* shift of pRFs is equivalent to a progressive *backward* shift of the corresponding population response over the same time and distance (the saccade size) (20). This backward shift of the population response effectively subtracts the saccade vector from a stimulus' presaccadic retinal position to produce its correct postsaccadic retinal position (Fig. 1*B*).

The entire remapping time course must be driven by CDs because the stimuli for measuring the pRFs are flashed before the saccade onset and there are no additional reafferent contributions to the pRFs during or after the saccade (8). This implies that the entire pRF remapping time course, including the portion after the saccade, can be viewed as predictive, and that what is remapped is the memory representations of the flashed stimuli. Then, to implement the above updating theory in a circuit model, we need a set of connections to maintain in memory the population response representing the retinotopic position of a flashed stimulus, and another set of connections, gated by the CD of a saccade, to shift the population response, across the saccade, to the updated position. We proposed the required connectivity patterns when modeling RF remapping in LIP and FEF (8). There are actually two types of RF remapping: the forward (or predictive) remapping discussed above and attentional (or convergent/compressive) remapping, which is RF shifts toward attended loci such as the saccade target or the fixation point (8, 21–23). Inspired by related models for orientation-tuning dynamics (24, 25), we explained attentional remapping with symmetric, center-excitation/surround-inhibition connections among cells tuned to different retinotopic locations (red curve of Fig. 2*A*). This so-called Mexican-hat connectivity pattern is consistent with interactions among cells in LIP (26) and FEF (27), and also provides attractor dynamics for maintaining responses in memory (28, 29). We explained forward remapping with CD-gated directional connections (blue curve of Fig. 2*A*) that propagate responses backward from cells' fRFs to their cRFs (8, 16). These two sets of connections form a complete circuit for transsaccadic spatial updating to achieve TSVS (8). Fig. 2*B* illustrates the updating of the second target across the first saccade of the double-step task (Fig. 1). The circles represent different cells' cRF centers (in retinotopic coordinates). The second target (diamond) appeared at the magenta cell's cRF center, evoking a population

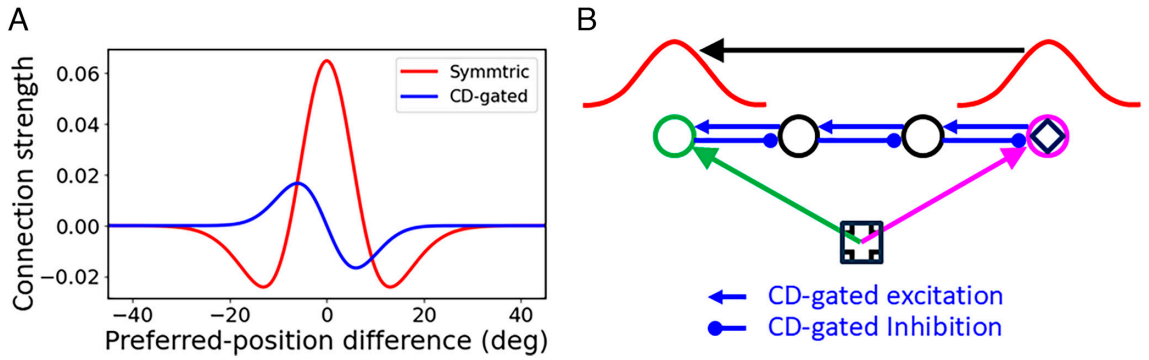

Fig. 2. A circuit model for RF remapping and population-response updating across saccades. (*A*) Recurrent connection strengths among model LIP/FEF cells as a function of the difference between the cells' preferred retinotopic positions (cRF centers). Symmetric, center-excitation/surround-inhibition connections (red) form memory for a flashed stimulus, and directional connections (blue, for rightward saccades) are gated by CDs to update the memory. (*B*) Schematic of the backward updating of the second target (diamond) across the first saccade of the double-step task of Fig. 1. Circles indicate a few cells' cRF center locations in retinotopic coordinates. The subject will make a saccade which will bring the diamond, now in the cRF of the magenta cell, into the cRF of the green cell. The diamond appears at the cRF center of the magenta cell, evoking a population response among nearby cells (red curve above the magenta cell) which is sustained by the symmetric connections (red curve in panel *A*) as a memory. This population memory response is shifted backward (black arrow) as a traveling wave when the CD activates directional connections between cells whose RF centers are between the magenta and green cells (blue lines), driving the cells as if the diamond had appeared in their cRFs, ultimately arriving at the green cell, which now will respond to the stimulus in its fRF on the screen. As the wave progresses, the intermediate cells will be activated with progressively longer delays, as observed in the forward remapping time course (8, 16).

response among the nearby cells (the red curve above the magenta cell) which is sustained by the center/surround connections (red curve in Fig. 2*A* not drawn in Fig. 2*B* to avoid clutter) as a memory. Across the first saccade, this response profile is continuously shifted backward by the CD-gated connections (blue curve in Fig. 2*A* and blue lines in Fig. 2*B*) to become a population response among the cells around the green cell (the red curve above the green cell), representing the updated retinotopic position of the second target. The total shift accumulated over time is equivalent to a subtraction of the saccade vector.

We also showed that the same circuit can update retinotopic positions of *persistent* stimuli across saccades (8). However, although persistent objects in daily life appear stable across saccades, we mislocalize brief stimuli flashed around saccades, relative to those flashed well before or after the saccades, a phenomenon known as perisaccadic perceptual mislocalization (30–32). The errors can be as large as many degrees of visual angle. If such errors occurred in daily life, our perception would be disturbingly unstable as objects would appear displaced after each saccade and then return to their correct positions when reafferent retinal inputs reach perception. Perisaccadic mislocalization has two components, a translational (or shift) component along the saccade axis and a convergent (or compressive) component toward the saccade target (31, 33). The convergent component is smaller and larger, respectively, in the absence and presence of a postsaccadic visual reference, such as a ruler (34). The translational mislocalization is in the saccade direction (forward) around the beginning of the saccade, and disappears, or sometimes reverses the direction (backward), around the end of the saccade (31, 32, 34).

We argued previously that RF remapping alone cannot explain the observed mislocalization (20). We now demonstrate that under additional and reasonable assumptions, our circuit model of RF remapping, which correctly updates persistent stimuli (and stimuli flashed well before or after saccades) for TSVS, will produce the observed translational mislocalization for stimuli flashed around the time of the saccade. We focus on translational mislocalization because convergent mislocalization is likely related to attention, a process distinct from transsaccadic updating and TSVS (8, 22, 35) (*Discussion*). The model makes testable predictions, and we confirmed one of them by reanalyzing our previous single-unit data from LIP and FEF (8). Our work clarifies, at the circuit level, the relationships among the physiological properties of RF remapping, the functional requirement of transsaccadic space updating, and the psychophysical observations of perisaccadic mislocalization, with implications on the nature of positional decoders used in the brain. The work suggests that translational mislocalization is really postsaccadic memory mislocalization of perisaccadically flashed stimuli. We presented the results previously at a conference (36) and as a preprint (37).

Results

We consider a typical paradigm for perisaccadic perceptional mislocalization: A subject makes a horizontal 12° saccade from an initial fixation point at −6° relative to the screen center to a target at +6° relative to the screen center while a probe stimulus is flashed at various times relative to the saccade onset; the location of the probe stimulus is reported after the saccade. Fig. 1*A* can be reinterpreted as a configuration for measuring mislocalization, with the cross and square representing the initial fixation and target positions, respectively, and the diamond representing the flashed probe stimulus. For translational mislocalization the location of the flash does not matter; we assume the flash is at the screen center (0°) and its retinotopic position changes with the eye position at the time of the flash. For horizontal saccades, we need to consider only the horizontal spatial dimension in our simulations.

The circuit model consists of a one-dimensional array of LIP/FEF units representing the horizontal retinotopic space (8). The units receive feedforward inputs originating from the retina and are recurrently connected to receive lateral input from each other. A flashed spot on the retina can be viewed as a delta function in space and time. When this input reaches the recurrent, LIP/FEF units, we represented it as a Gaussian function in space and a gamma function in time to account for the intervening low-pass spatiotemporal filtering which produces spatial smear and temporal delay. The recurrent connections among the units are translationally invariant (38) and can be divided into two sets. The first set follows a symmetric, center-excitation/surround-inhibition pattern among units tuned to different retinotopic positions (Fig. 2*A*, red curve). The second set is antisymmetric, directional connections gated by the CD of the saccade command with excitation and inhibition in the backward and forward directions, respectively (Fig. 2*A*, blue curve for rightward saccades). Since the

physiological data show that forward RF remapping starts about 100 ms before the saccade onset and continues up to 100 ms after the saccade offset, we chose a similarly broad CD time course (Fig. 3, third row). The details of the model and its parameterization can be found in *Methods*; the model works with many different combinations of parameters (8).

We first considered the case when the stimulus is flashed 295 ms before the saccade onset (Fig. 3*A*; flash time indicated by the green line in the third panel). Despite delay from the retina to LIP/FEF (39), the input reaches the LIP/FEF units (first panel; red curve, third panel) before the start of the CD signal (black curve, third panel). This input pattern is processed by the symmetric recurrent connections to produce a population response profile that stores the stimulus retinotopic position as a memory (second panel) (8). We used the center-of-mass location of the response profile at a given time as the decoded retinotopic position of the stimulus at that time (red curve, fourth panel). When the saccade CD emerges, the memory response profile, and thus the decoded position, is updated backward by the CD-gated directional connections. We chose the CD strength such that the final, cumulative updating after the saccade is equal to the negative saccade vector (from retinotopic 6° to −6°, a total of −12°). Although the sluggish CD time course creates a mismatch between the ideal and the actual updating time courses, the finally updated retinotopic position, which stabilizes about 150 ms after the saccade offset (or 200 ms after the saccade onset), is accurate.

We next simulated how the same model responds to the stimulus flashed at the saccade onset (Fig. 3*B*). Because of the response delay from the retina to LIP/FEF and the CD signal starts before the saccade onset, by the time the input reaches the LIP/FEF units, it has missed much of the CD time course. Consequently, the cumulative backward updating of the memory response profile after the saccade is far short of the saccade size, resulting in a positional error in the forward direction (Fig. 3*B*).

We then considered the case when the stimulus is flashed at the end of the saccade (Fig. 3*C*). Because the flash occurs when the eye has almost stopped moving, ideally there should be little updating of the retinotopic position of the stimulus. However, despite the response latency, the input to the LIP/FEF units still catches a tail part of the sluggish CD time course, and consequently the memory response profile is shifted backward slightly, producing a small positional error in the backward direction (Fig. 3*C*).

Fig. 4*A* summarizes the cumulative backward updating of the flash's retinotopic position after the saccade as a function of the flash time relative to the saccade onset (red curve, *Top* panel). Its difference from the ideal cumulative updating (purple curve, *Top* panel) is the mislocalization (black curve, *Bottom* panel), which explains the translational component of the observed perisaccadic mislocalization. To explore the effect of the response latency from

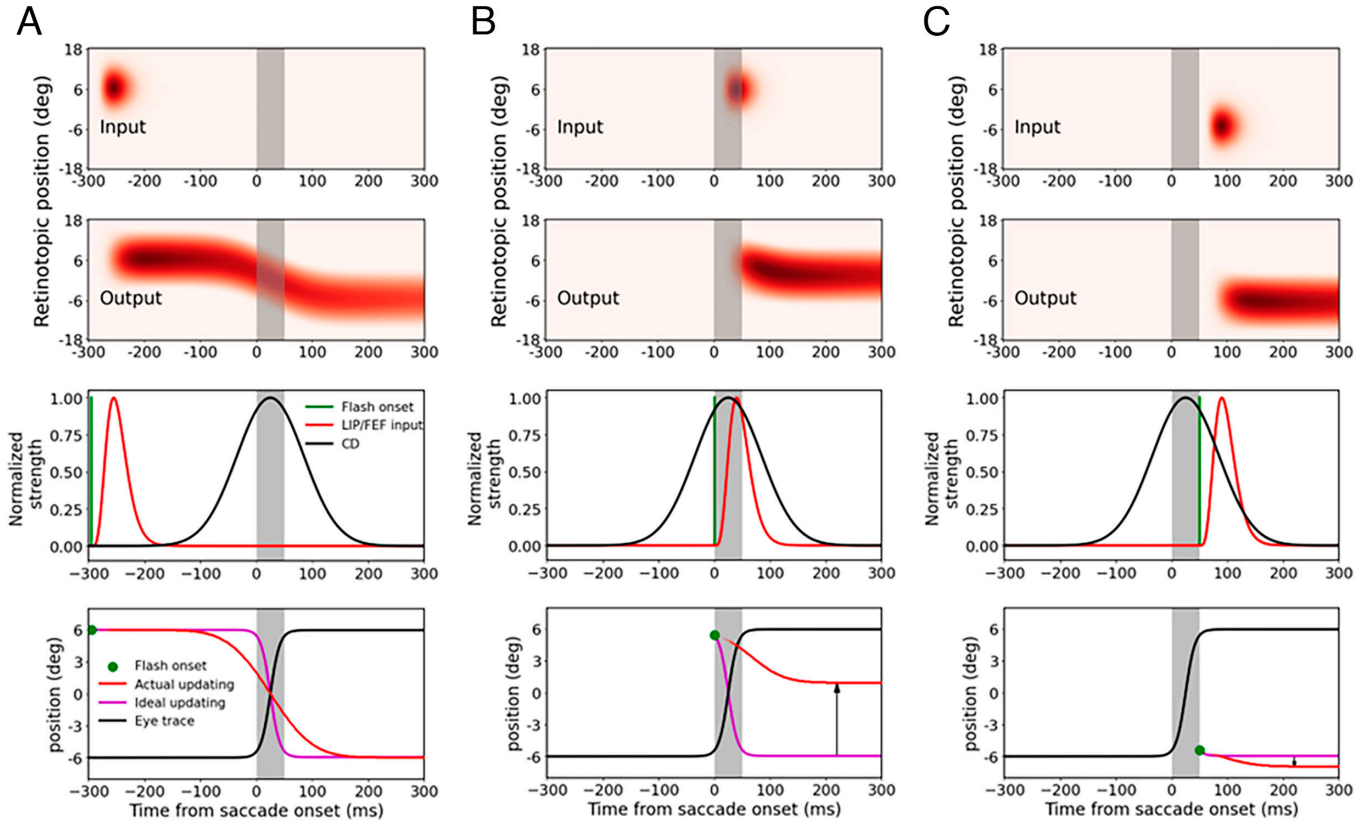

Fig. 3. The circuit model explanation of translational mislocalization of stimuli flashed around saccades. The saccades are 12° rightward from −6° to +6° and the flashes are at 0° relative to the screen center. The gray shades indicate the 50-ms saccade duration. The three columns are the simulation results for the flash at (*A*) 295 ms before saccade onset, (*B*) saccade onset, and (*C*) saccade offset, respectively. The first and second rows show the heatmaps of the input to, and output from, the LIP/FEF units as a function of the units' retinotopic RF positions (*y* axis) and time (*x* axis). The horizontal space is shown vertically to be consistent with Fig. 4 and the convention used in many mislocalization studies. The third row shows the temporal relationships of the flash on the retina (green), the input of the flash to the LIP/FEF units (red), and the CD signal (black), with the peaks normalized to 1. The delay from the retinal flash to the peak of LIP/FEF input is 40 ms. The fourth row shows the time course of the eye position (black) in the craniotopic coordinate (relative to the screen center), and the ideal (purple) and actual (red) updating of the flash's position (green dot) in the retinotopic coordinate (relative to the fovea/fixation). The actual updating curves (red) are the center-of-mass of the output population responses in the second row. The ideal updating has the inverted shape of the eye position trace. The final differences (vertical arrows) between the cumulative actual and ideal updating after the saccade (any time after about 200 ms) are the mislocalization. The upward and downward arrows indicate forward and backward mislocalization for flashes at the saccade onset and offset, respectively.

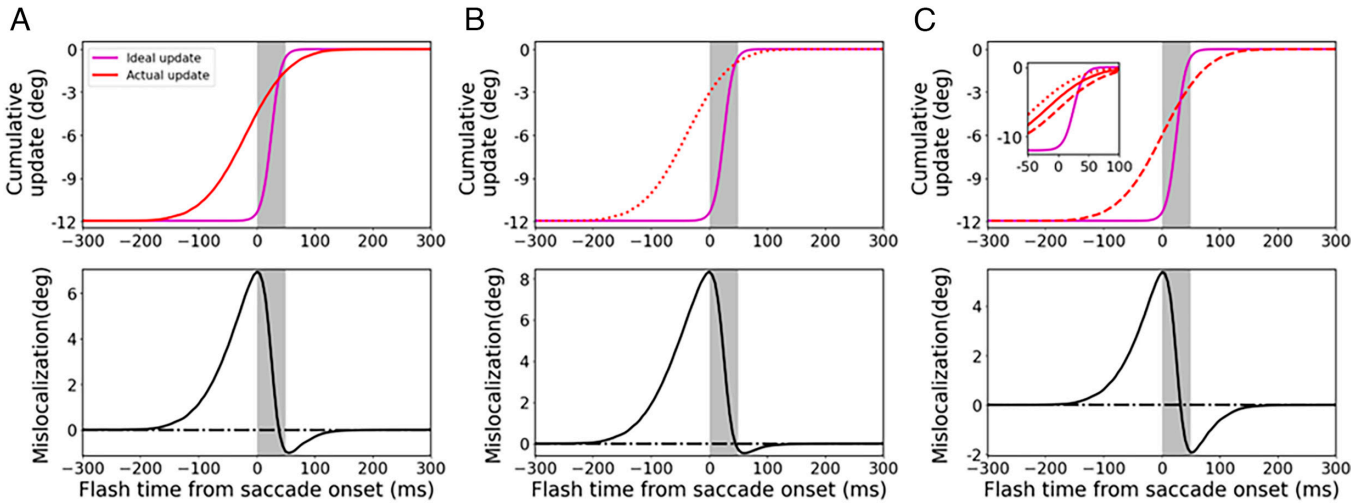

Fig. 4. Postsaccadic cumulative updating and mislocalization for stimuli flashed at different times relative to the saccade onset. The three columns show results obtained with (*A*) the same parameters as in Fig. 3, (*B*) the delay from the retinal flash to the peak of LIP/FEF input increased by 20 ms (to 60 ms), and (*C*) the CD profile delayed by 20 ms (equivalent to decreasing the retina-to-LIP/FEF delay by 20 ms). The *Top* row shows the actual (red) and ideal (purple) cumulative updating of the flash's retinotopic position after the saccade, and the *Bottom* row shows their difference, the postsaccadic memory mislocalization. The ideal cumulative updating is the negative of the eye-position change from the time of the flash to the end of the saccade. The *Inset* in (*C*) compares the three actual updating curves (red solid, dotted, and dashed), which are only separated by 20 ms, for the three cases.

the retina to LIP/FEF, we shifted the gamma temporal response profile rightward by 20 ms so that the delay from retinal flash to the peak LIP/FEF input increases to 60 ms. As can be seen from the results in Fig. 4*B*, the forward and backward mislocalization of the flashes around saccade onset and offset becomes larger and smaller, respectively, with the longer input delay. This is expected because a longer input delay increases the missed portion of the CD time course which makes the backward updating of the flash around the saccade onset even more insufficient (i.e., larger forward mislocalization) and the unnecessary updating for the flash around the saccade offset smaller (i.e., smaller backward mislocalization). Conversely, if we reduce the response latency, or equivalently, if the CD profile is later than what we assumed in Fig. 3*A*, then the forward and backward mislocalization for the flashes around the saccade onset and offset will become smaller and larger, respectively (Fig. 4*C*). (The red updating curves in the three panels of Fig. 4 are shifted from each other by only 20 ms; the *Inset* in panel *C* shows them together to emphasize their differences.) One way to manipulate the response latency is to change the stimulus contrast or size (*Discussion*). Overall, the simulations are consistent with the observation that the forward mislocalization around the saccade onset is usually larger in magnitude, and more robust across studies, compared with the backward mislocalization around the saccade offset (30, 32, 34).

We finally applied the same model to a persistent stimulus and the result is shown in Fig. 5. The final, cumulative updating of its retinotopic position after the saccade is accurate, similar to the updating of the flash well before the saccade in Fig. 3*A* (see also ref. 8). This result ensures that for a persistent stimulus with a fixed position in the world, its presaccadic retinotopic position is updated to the postsaccadic retinotopic position that agrees with the reafferent retinal input position from the same stimulus after the saccade. We suggest that this agreement achieves TSVS for persistent objects in daily life.

Our model makes a few predictions (*Discussion*), one of which is the updating curves (red) in the *Bottom* row of Fig. 3 and the *Top* row of Fig. 4. They show that the later the flash, the smaller is the magnitude of the backward updating of the population response to the flash. It is particularly interesting to focus on flashes before the saccades because their retinotopic positions should all be updated backward by the saccade size (purple curves at −12° before 0 time in Fig. 4) but the actual updating magnitude gets smaller as the flash gets closer to the saccade onset. This is equivalent to the prediction that for perisaccadic RFs measured with flashes before the saccades, the remapping magnitudes are smaller for later flashes (20). We reanalyzed our previously published single-unit data from LIP and FEF (8) to test this prediction. We first compiled the distributions of the perisaccadic flash time relative to the saccade onset for the LIP cells and FEF cells (Fig. 6*D*). Since the median times for both areas are around −100 ms and the red curves of Fig. 4 suggest that flashes earlier than −100 ms are fully (−12°) or almost fully updated whereas later flashes start to show insufficient updating, we used the −100 ms time to divide a given cell's trials at each probe location into early and late categories. Finally, we applied the same procedure as in ref. 8 to determine the time course of the pRF remapping magnitude but for the early and late trials separately. Since the remapping direction is largely forward from around saccade onset to about 350 ms afterward (*SI Appendix*, Fig. S1), we focused on this period. The remapping magnitude is the distance between a cell's pRF center (determined from its responses in a 50-ms window centered at a given time) and its cRF center, and the time is measured relative to the saccade onset (regardless of the response onset times). [We did not use a time relative to the stimulus or response onset because forward shift depends on saccade CDs (40). We previously used times relative to the stimulus onset as well as to the saccade onset when studying both forward and attentional (convergent) remapping (8)].

Panels *A*–*C* of Fig. 6 show the average results from LIP, FEF, and the two areas combined, respectively. The mean remapping magnitudes are indeed greater for the early-flash trials (red) than for the late-flash trials (blue) most of the time. To avoid accumulation of type I errors of multiple comparisons, we performed a single ANOVA test with the early-late categories and eight nonoverlapping time bins as repeated-measure factors (because a given cell's remapping values under these 2 × 8 conditions are not independent) and the brain area as a predictor. First, there is no significant difference between LIP and FEF [$F(1) = 0.85$, $P = 0.36$], which justifies pooling the data of the two areas. Second, there is a significant difference between the early and late categories [$F(1) = 6.3$, $P = 0.013$] confirming our prediction. The difference is

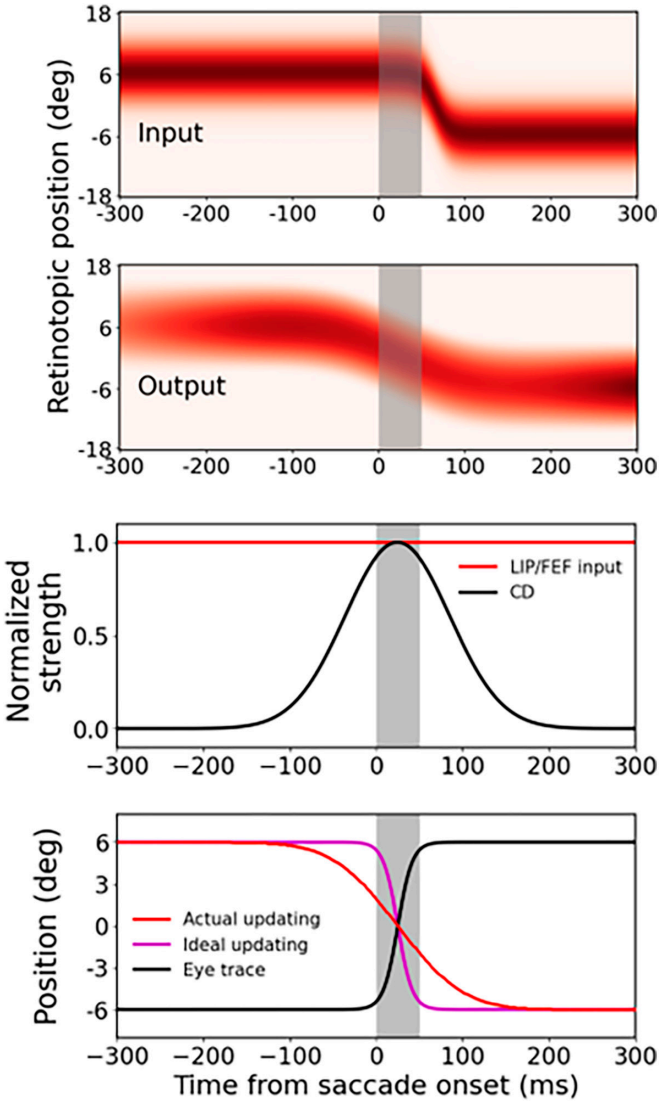

Fig. 5. Transsaccadic updating of a persistent stimulus by the circuit model. The model parameters and the presentation format are the same as those for Fig. 3*A* except that the stimulus is always on at the screen center and its input to the LIP/FEF units is delayed by 40 ms (first row). The cumulative updating of the stimulus' retinotopic position after the saccade (e.g., after 200 ms) is accurate.

small; this is expected because the flash time distributions *peak* around 100 ms before the saccades, and among the late half trials, not many had the flashes close to the saccade onset (Fig. 6*D*) when the most deficient remapping/updating occurs (Fig. 4). The physiological experiment was not designed for this test but we still found the predicted effect. Third, there is a significant difference across the time bins [$F(7) = 61$, $P = 8.5 \times 10^{-77}$]. Indeed, the initial increase of the remapping magnitudes for all the curves indicates the gradual forward shift of the pRFs with time (8). Finally, there is no significant interaction between the early-late category and the time bins [$F(1, 7) = 0.68$, $P = 0.69$]. The early- and late-trial curves overlap sometimes, which is *not* predicted by the model. The lack of significant interaction suggests that the overlaps likely reflect the noise in the data. The noise effect must be increased by splitting trials into the early and late categories but decreased by pooling the LIP and FEF data. On the other hand, the early- and late-trial curves have overlap for both LIP and FEF about 120 ms after the saccade onset. Whether or not this point reflects some real physiological processes not captured by the model requires further investigation.

Discussions

We argued previously that RF remapping *alone* cannot explain the observed perisaccadic perceptional mislocalization (8, 20). First, when converting RF remapping into the corresponding population response for positional decoding, it is unclear whether the decoders should consider the population response as a function of each cell's remapped RF position (pRF center), thus aware of the remapping, or the original RF position before the remapping (cRF center), thus unaware of the remapping. The aware case produces no shift of the population response, and the unaware case produces a backward shift of the population response. Second, there is a mismatch between remapping studies and mislocalization studies: The former present perisaccadic stimuli before the saccade onset and measure RF shifts at different times across the saccade whereas the latter present a stimulus at different times across the saccade and measure its perceived position after the saccade. In this paper, we demonstrate that under some additional assumptions, which address the above two issues, the circuit model that uses CD-driven remapping/updating to achieve TSVS can explain the translational component of the observed mislocalization.

Our first assumption is that the forward remapping of retinotopic RFs is the sole mechanism for transsaccadic space representation over a few hundred ms around a saccade. This assumption is used in our simulations above as we decoded stimulus position solely from the updated retinotopic responses without considering craniotopic contributions. The assumption is consistent with the evidence that the CD-based remapping/updating mechanism operates even before a single saccade, and the eye-position-based craniotopic mechanism is inaccurate for at least 150 ms after a saccade (41). The assumption also implies that the brain must use unaware positional decoders with which the forward RF remapping is equivalent to the backward shift (updating) of the corresponding population response to achieve TSVS (20). In contrast, with aware decoders, forward RF remapping is not equivalent to a backward shift of the population response and cannot be the mechanism for transsaccadic space updating.

To see the difference between aware and unaware decoders intuitively, consider the green cell in Fig. 2*B* which can be activated by either 1) the stimulation of its cRF or 2) the stimulation of the magenta cell's cRF and then the lateral propagation of the activity from the magenta cell to the green cell via the CD-gated directional connections. For unaware decoders, the green cell's activity is always evidence for a stimulus positioned at its cRF regardless of where that activity originates. For aware decoders, however, the green cell's activity is evidence for a stimulus positioned at the green and magenta locations for the two cases, respectively. In other words, unaware decoders treat a cell as a fixed, labeled line whereas aware decoders "know" the origin of a cell's activity and interpret it accordingly. Obviously, it would be much easier for the brain to implement unaware decoders than aware decoders but ultimately, this is an empirical issue to be settled by future experiments. Adaptation aftereffects provide indirect evidence for unaware decoders because aware decoders would know the adaptation-induced change of neuronal responses and could null the aftereffects in principle (42–44). Similarly, experiments showing perceptual shifts of position after inducing RF shifts in the absence of eye movements support the use of unaware decoders in the brain (45, 46).

Our second assumption is that in perceptual mislocalization experiments, the reported position of a flash is not decoded from the responses when they first reach LIP/FEF, but rather from the responses *after* the saccade, i.e., at the time of the report. For

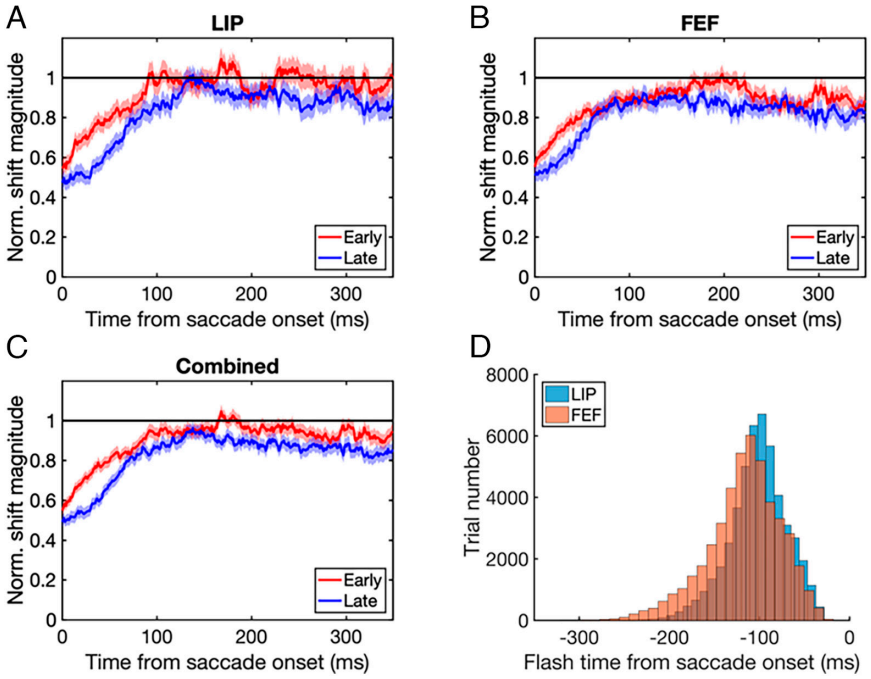

Fig. 6. Testing the model prediction that for pRFs measured with flashes before the saccades, the forward remapping magnitudes are smaller for later flashes. (*A*–*C*) The time courses of the mean forward remapping magnitudes in LIP, FEF, and the combined data for the early (red) and late (blue) trials. The remapping magnitude is normalized by the corresponding saccade size before averaging over the cells. The horizontal line at 1 indicates a remapping magnitude equal to the saccade size. The shaded region around each mean curve indicates ±1 SEM. (*D*) The distribution of the flash onset time relative to the saccade onset for the LIP and FEF cells. The numbers of the cells are n = 104 and 113 for LIP and FEF, respectively.

example, Fig. 3*A* shows that when a stimulus is flashed well before a saccade, the decoded position before the saccade onset would predict a backward mislocalization (20), but the decoded position *after* the saccade shows no mislocalization. Alternatively, we could assume that the reported perception is the time average of the decoded screen position of the flash up to the report time. Note that the ideal retinotopic curves (purple) in the *Bottom* row of Fig. 3 correspond to the correct, fixed flash position on the screen (the screen center). Thus, the mislocalization predicted by the alternative assumption is simply the average difference between the actual (red) and ideal (purple) curves in Fig. 3. This average would be zero (no mislocalization), positive (forward mislocalization), and negative (backward mislocalization), respectively, for the flashes well before the saccade, around the saccade onset, and around saccade offset, similar to the results in Figs. 3 and 4. Again, future studies are needed to evaluate these assumptions. Our work suggests that perisaccadic perceptual mislocalization is actually postsaccadic memory mislocalization of perisaccadically flashed stimuli, lending further support to the notion that perceptual decoding often occurs in working memory (47, 48).

Our final assumption is that persistent stimuli (and similarly, brief stimuli flashed well before saccades) are updated correctly across saccades without mislocalization (20, 49). This can be viewed as a definition of TSVS because, as we noted earlier, it ensures that for an object with a fixed position in the world, its presaccadic retinotopic position is updated to the postsaccadic retinotopic position that agrees with the reafferent retinal input from the same object after the saccade. Subjects may have individual biases in positional judgments unrelated to saccades, but those biases simply set the baseline against which perisaccadic mislocalization is determined. We thus did not consider such biases in our model.

In addition to the above assumptions, we also incorporated the following two facts into the model. First, the forward remapping in LIP and FEF has a sluggish time course that starts a little before the saccade onset and ends a little after the saccade offset (8). We assumed a correspondingly sluggish CD signal to drive the remapping/updating in the model. Second, there is a response latency from the retina to the remapping/updating stages such as LIP/FEF (16). We implemented the delay via low-pass temporal filtering and/or a hard time shift (50). Because of the sluggish CD signal and the visual response latency, stimuli flashed at the saccade onset, whose retinotopic position should be updated backward by the saccade size after the saccade, would miss part of the CD time course, leading to insufficient backward updating and hence forward mislocalization. Stimuli flashed at the saccade offset, whose retinotopic position should not be updated, might still catch the tail of the CD time course, producing an unnecessary backward updating or backward mislocalization.

As we already noted, our model predicts that for pRFs measured with flashes before the saccade, the forward remapping magnitudes are larger for earlier flashes. We reanalyzed our previous single-unit data from LIP and FEF and confirmed this prediction (Fig. 6). This result also partially explains the observation that the final forward remapping magnitude after the saccade is a little smaller than the saccade size (8) as some of the flashes for measuring pRFs must have missed part of the CD time course. [An additional explanation is that RFs of LIP and FEF cells are not strictly retinotopic (4)]. Another prediction of the model is that when the response delay from the retina to the stages of updating (LIP/FEF) is increased, the forward and backward translational mislocalization of flashes around the saccade onset and offset will become larger and smaller, respectively (Fig. 4). This could be tested by varying stimuli's contrast and size: Stimuli with greater contrast and optimal size should have shorter response latency and therefore produce larger forward and smaller backward translational mislocalization of flashes around the saccade onset and offset, respectively. There is also a corresponding physiological prediction: For stimuli flashed at the same time right before the saccade, those evoking shorter-latency responses should have larger forward remapping

magnitudes. Although our circuit model is one-dimensional and one directional, which is sufficient for simulating mislocalization during rightward saccades, it can easily be expanded to two spatial dimensions with different saccade directions (8).

Many ingredients of our model have been proposed previously but to our knowledge, they have never been integrated into a circuit model of RF remapping and TSVS to explain perisaccadic mislocalization. Early studies posit that during a saccade, the brain has a sluggish estimate of the eye position that first leads but then lags the actual eye position, producing forward and backward mislocalization around the saccade onset and offset, respectively (30, 31). However, the only known cortical representation of eye position (separable from the position of a saccade target) is the proprioceptive representation of eye position in Area 3a (51), arising from sensors in the eye, and lags the actual eye position by an average of 60 ms (52). Pola (53) shows that when latency and persistence of visual responses to flashed stimuli are considered, a delayed but otherwise veridical eye-position estimate can account for the translational mislocalization. Teichert et al. (49) demonstrate that with physiological temporal filtering of visual inputs, the eye-position estimate that eliminates mislocalization for persistent stimuli produces translational mislocalization for flashed stimuli. Although we also include a sluggish signal (CD) and temporal filtering/delay, our model does not use an estimate of the eye position but instead, updates the stimuli's retinotopic position, across saccades. More importantly, our model and the previous models assume that mislocalization arises from the stimulus memory *after* the saccade and the eye-position estimation *during* the saccade, respectively. In a preprint, Berreby and Krishna (54) also used our circuit model (8, 36, 37) to explain mislocalization (see ref. 37 for a discussion of the 2023/2024 versions of their preprint). Our results cannot be derived from the forward RF remapping alone (20) but depend on the assumptions and facts discussed above.

Early remapping studies found that some cells responded to stimuli in their fRFs even before the saccade onset (6, 15). Because the detailed RF profiles were not measured, it is unknown whether these cells' pRFs *completely* shifted from their cRF to fRF locations (i.e., a center-to-center shift equal to the saccade vector) *before* the saccade. Given the large RF sizes, a partial shift would also be consistent with the data. If the complete RF shift did occur before the saccade [and the cells' RFs return to their normal, retinotopic locations after the saccade (4)], then the cells' pre- and postsaccadic RF locations on the screen would be identical and, in this sense, the cells would be transiently craniotopic (55). However, later, more detailed RF measurements in LIP and FEF showed that near-complete forward shift occurred much later, about 100 ms *after* the saccade on average (8), a finding used in this paper. Future studies are needed to examine whether transient craniotopy is a mechanism for TSVS in other brain areas.

RFs that progressively shift forward in space over time across saccades (8, 16) are spatiotemporally oriented (20, 55–58). Thus, forward-remapping cells (with nonlinearities after spatiotemporal filtering) may be viewed as CD-dependent, high-speed motion detectors which detect saccade-induced retinal motion. The process computes spatiotemporal correlations of retinal inputs and may determine the correspondence between pre- and postsaccadic retinal images to achieve TSVS. However, it is unclear how to apply this motion model to brief stimuli flashed well before saccades as there is no saccade-induced retinal motion. In contrast, our updating model can properly update the *memory* activities of such stimuli from their pre- to postsaccadic retinotopic locations [Fig. 3*A*, (8)]. For persistent stimuli, the motion model needs to account for the retina-to-LIP/FEF delay because it depends on saccade-induced retinal motion whereas the updating model is largely unaffected by the delay [Fig. 5, (8)] because it updates the activities already reached LIP/FEF before saccades. Additionally, the sluggish remapping time course that starts before and ends after the saccade (8) implies that forward-remapping cells are tuned to speeds smaller than the saccade-induced retinal speeds, and the motion model must tolerate this mismatch during motion detection. The two models are not mutually exclusive, and both mechanisms may contribute to TSVS of persistent stimuli in the real world.

While most studies found forward mislocalization for stimuli flashed around the saccade onset, two studies reported backward mislocalization instead (59, 60). A key difference between these two studies and the rest is that the former provided veridical feedback of the flash position at the end of each trial whereas the latter did not. Why the feedback does not just eliminate or reduce the forward mislocalization but somehow overcompensates to produce the backward mislocalization is an open question. One possibility is that subjects might exaggerate the difference between the perceived stimulus position and the feedback position, as in many perceptual repulsion phenomena (47, 61), which could lead to overcompensation through the feedback-driven learning.

We focused on the translational component of perisaccadic mislocalization. How, then, can the convergent or compressive component of the mislocalization be explained? We previously analyzed how various factors may affect convergent vs. divergent mislocalization (20), but if we assume that the brain uses unaware decoders, as we argued above, then we only need to consider attentional enhancement of responses around the saccade target, and convergent (compressive) RF shifts toward the target (attentional RF remapping). [The notion that attentional RF remapping increases the cell density covering the attentional locus is only true under the aware-decoder assumption (20)]. The attentional enhancement of responses alone "pulls" stimulus-evoked population responses toward the target whereas the attentional RF remapping alone "pushes" the population responses away from the target. The net effect of the two factors could be either convergent or divergent mislocalization depending on their relative strengths and the stimulus distance from the target (20). However, the two factors may not be independent: Attentional response modulation at the target may produce attentional remapping toward the target (8), and their quantitative relationship depends on the parameters of the center/surround connections. Additionally, different studies found very different strengths of attentional remapping (8, 22). Moreover, there are also psychophysical reports of perceptual repulsion away from attentional loci, namely, divergent mislocalization (62–64). Finally, attentional allocation to the target may vary with time across saccades (8). Further studies are needed to resolve these issues.

Mislocalization of flashed stimuli similar to perisaccadic mislocalization has been produced by simulating saccade-like retinal motion but without the actual saccade (65, 66). Such motion induced mislocalization of flashed stimuli in the absence of eye movements is known as the flash-lag effect (67, 68). This raises the possibility that perisaccadic mislocalization and the flash-lag effect might share similar underlying mechanisms (20, 49). Interestingly, motion can enhance lateral connections, in the motion direction, among cells tuned to different positions via spike timing–dependent plasticity (46), similar to the CD gated lateral connections in our model. If the motion-enhanced connections are the mechanism for predictively updating the retinotopic positions of moving stimuli, then a circuit model similar to ours might explain the flash-lag effect. Future studies will hopefully clarify the relationships between

different mislocalization phenomena and improve our understanding of neural mechanisms of space perception.

Methods

Circuit Model. We simulated a one-dimensional array of 360 LIP/FEF units covering 180° of horizontal retinotopic space, each unit governed by the equations:

$$\tau \frac{\partial u(x,t)}{\partial t} = -u(x,t) + \sum_{x'} W(x,x') r(x',t) dx' + I(x,t),$$

$$r(x,t) = max(u(x,t), 0),$$

where $u(x,t)$ and $r(x,t)$ represent, respectively, the membrane potential and firing rate of the unit at location and time (x,t), τ is the membrane time constant, $W(x,x')$ is the recurrent connection strength from neuron at x' to neuron at x and depends on $(x-x')$ only, and I is the feedforward inputs to LIP/FEF which originate from the retina. $W(x,x')$ is a sum of two parts: 1) symmetric, center-surround connections modeled as a weighted difference between two Gaussians: $J_{exc}G(x,x',\sigma_{exc}) - J_{inh}G(x,x',\sigma_{inh})$ where $G(x,x',\sigma) = \left(-\frac{(x-x')^2}{2\sigma^2}\right)$, and 2) directional connections gated by the saccade CD, with the excitation and inhibition in the backward and forward directions of the saccade, respectively. For the simulations in this paper, we let $J_{exc} = 0.165$, $\sigma_{exc} = 6°$, $J_{inh} = 0.1$, $\sigma_{inh} = 9.6°$. For rightward saccades, we modeled the CD-gated connections as the antisymmetric, spatial derivative of the first Gaussian part of the center-surround connections: $J_{cd}(t)\frac{\partial J_{exc}G(x,x',\sigma_{exc})}{\partial x}$ where the CD gating factor $J_{cd}(t) = J_{cdm}\ exp\left[-\frac{1}{2}\left(\frac{t-t_m}{\sigma_{cd}}\right)^2\right]$ and t_m is the mid time of the saccade duration assumed to be 50 ms. For the simulations in Fig. 4*C*, we shifted $J_{cd}(t)$ to the right by 20 ms. We let $\sigma_{cd} = 60$ ms, $J_{cdm} = 0.97$. The blue curve of Fig. 2*A* shows the maximum directional connections when $t = t_m$. Note that we previously used a CD time course that matches the saccade duration because we trained neural networks to do ideal updating of retinotopic positions (8). Here we used a sluggish CD time course that matches the average RF remapping time course in LIP/FEF and is broader than the saccade duration.

We considered both flashed and persistent visual inputs. A spot flashed on retina is filtered both spatially and temporally when it reaches LIP/FEF so we modeled its input to LIP/FEF units as a spatial Gaussian function and a temporal gamma function:

$$I(x,t) = J_{in}G(x,x_0,\sigma_{in})f(t,a,b),$$

$$f(t,a,b) = \frac{1}{b^a\Gamma(a)}t^{a-1}e^{-t/b},$$

where x_0 is the retinotopic position of the flash, and a and b are the shape and scale parameters, respectively. Translational mislocalization does not depend on the flash position. For the plots, we arbitrarily assumed a flash position of 0 in the screen coordinate; its retinotopic position varies with the eye position and is +6° and −6° before and after the 12° saccade, respectively. We let $\sigma_{in} = 4°$, $J_{in} = 4$, $a = 6$, $b = 8$ ms so the delay from the retinal flash to the peak of the LIP/FEF input is $(a-1)b = 40$ ms. For the simulations in Fig. 4*B*, we added an additional delay of 20 ms by shifting the gamma function to the right by 20 ms so the total delay is 60 ms. We also considered a persistent stimulus turned on long before the saccade onset and stayed at the screen center throughout. During the saccade, the Gaussian spatial profile of this input to the LIP/FEF units changes its retinotopic position according to the eye position and in the simulation (Fig. 5), this change is delayed by 40 ms to account for the visual response latency.

Analysis of LIP and FEF Single-Unit Data. We reanalyzed our LIP and FEF single-unit data in a published study (8) to test the prediction that for pRFs measured with flashes before the saccades, the forward remapping magnitudes are smaller for later flashes. The details of the experimental design and data collection and analysis can be found in that publication. Briefly, we recorded single units from monkeys' LIP and FEF while they performed a delayed saccade task. For each unit, we measured its RFs from four different time periods (current, delay, perisaccadic, and future) by flashing a probe stimulus at one of the array locations in each period of each trial, and denote the RFs so measured as the cell's cRF, dRF, pRF, and fRF, respectively. For the current purpose, we focused on the cells' RFs measured from the perisaccadic period (pRFs) and compared the remapping of the pRFs derived from the trials with early and late flashes. We used the same 104 LIP cells and 113 FEF cells that passed our screening procedure under the saccade-onset alignment of repeated trials, and their cRFs and fRFs (8). For their pRFs, we previously excluded trials whose perisaccadic probe onset was after the saccade onset (8). Here, we used a slightly more stringent criterion by excluding trials whose probe offset was after the saccade onset. We compiled the distributions of the perisaccadic flash onset time relative to the saccade onset for all the LIP cells and all the FEF cells separately. Fig. 6*D* shows the results by dividing the time range of each brain area into 40 bins. Since the median times for both areas are around −100 ms relative to the saccade onset and the red curves of Fig. 4 suggest that flashes earlier than −100 ms are close to fully updated whereas later flashes start to show insufficient updating, we used the −100 ms time to divide a given cell's trials at each flash location into early and late groups. Because of the relatively small number of trials at each flash location, the trials for some locations of some cells may all belong to the early or late group. We used Matlab's scatteredInterpolant function with the "natural" method to fill in the missing mean responses at those locations. We then applied the same procedure as in ref. 8 to determine the time course of the pRF remapping but for the early and late trials separately (Fig. 6 *A* and *B*). Since the prediction we tested is about forward remapping, we examined the remapping direction (as well as magnitude) in LIP and FEF over an extended period from −50 to 400 ms relative to the saccade onset (*SI Appendix*, Fig. S1). The remapping direction is largely forward between 0 and 350 ms in both LIP and FEF, so we used this period in Fig. 6.

Data, Materials, and Software Availability. Single-unit data have been deposited in Mendeley Data (DOI: 10.17632/2p5vhm2w8n.1) (69). Previously published data were used for this work (10.17632/w6y53574zp.1) (70).

ACKNOWLEDGMENTS. Supported by National Natural Science Foundation of China (32030045, 42405195) and US National Eye Institute (R01 EY032938, P30 EY019007). We are grateful for the administrative help of Danielle Shank and Andrea Hurtado.

Author affiliations: [a]Division of Psychology, State Key Laboratory of Cognitive Neuroscience and Learning, International Data Group/McGovern Institute for Brain Research, Beijing Normal University, Beijing 100875, China; [b]Chengdu Fluid Dynamics Innovation Center, Chengdu, Sichuan 610017, China; [c]Bergen County Technical High School, Teterboro, NJ 07608; [d]Department of Neuroscience and Zuckerman Institute, Columbia University, New York, NY 10027; [e]Department of Neurology, Columbia University, New York, NY 10032; [f]Department of Psychiatry, Columbia University, New York, NY 10032; [g]Department of Ophthalmology, Columbia University, New York, NY 10032; and [h]Department of Physiology and Cellular Biophysics, Columbia University, New York, NY 10032

1. R. A. Andersen, G. K. Essick, R. M. Siegel, Encoding of spatial location by posterior parietal neurons. *Science* **230**, 456–458 (1985).
2. D. Zipser, R. A. Andersen, A back-propagation programmed network that simulates response properties of a subset of posterior parietal neurons. *Nature* **331**, 679–684 (1988).
3. J.-R. Duhamel, F. Bremmer, S. Ben Hamed, W. Graf, Spatial invariance of visual receptive fields in parietal cortex neurons. *Nature* **389**, 845–848 (1997).
4. L. Yang, M. Jin, C. Zhang, N. Qian, M. Zhang, Distributions of visual receptive fields from retinotopic to craniotopic coordinates in the lateral intraparietal area and frontal eye fields of the macaque. *Neurosci. Bull.* **40**, 171–181 (2024).
5. H. von Helmholtz, *Handbook of Physiological Optics* (Optical Society of America, New York, ed. 3, 1928), Translated by J. P. C. Southall.
6. J. R. Duhamel, C. L. Colby, M. E. Goldberg, The updating of the representation of visual space in parietal cortex by intended eye movements. *Science* **255**, 90–92 (1992).
7. M. A. Sommer, R. H. Wurtz, Influence of the thalamus on spatial visual processing in frontal cortex. *Nature* **444**, 374–377 (2006).
8. X. Wang *et al.*, Perisaccadic and attentional remapping of receptive fields in lateral intraparietal area and frontal eye fields. *Cell Rep.* **43**, 1–16 (2024).
9. M. Poletti, D. C. Burr, M. Rucci, Optimal multimodal integration in spatial localization. *J. Neurosci.* **33**, 14259–14268 (2013).
10. O. Rutler *et al.*, Mice require proprioception to establish long-term visuospatial memory. bioRxiv [Preprint] (2023). https://doi.org/10.1101/2023.10.03.560558 (Accessed 5 October 2023).

11. D. C. Burr, M. C. Morrone, J. Ross, Selective suppression of the magnocellular visual pathway during saccadic eye movements. *Nature* **371**, 511 (1994).
12. B. J. Richmond, R. H. Wurtz, Vision during saccadic eye movements. II. A corollary discharge to monkey superior colliculus. *J. Neurophysiol.* **43**, 1156–1167 (1980).
13. A. Thiele, P. Henning, M. Kubischik, K.-P. Hoffmann, Neural mechanisms of saccadic suppression. *Science* **295**, 2460–2462 (2002).
14. F. W. Campbell, R. H. Wurtz, Saccadic omission: Why we do not see a grey-out during a saccadic eye movement. *Vision Res.* **18**, 1297–1303 (1978).
15. M. M. Umeno, M. E. Goldberg, Spatial processing in the monkey frontal eye field.1. Predictive visual responses. *J. Neurophysiol.* **78**, 1373–1383 (1997).
16. X. Wang *et al*., Perisaccadic receptive field expansion in the lateral intraparietal area. *Neuron* **90**, 400–409 (2016).
17. N. So, M. N. Shadlen, Decision formation in parietal cortex transcends a fixed frame of reference. *Neuron* **110**, 3206–3215.e5 (2022).
18. T. B. Crapse, M. A. Sommer, Frontal eye field neurons assess visual stability across saccades. *J. Neurosci.* **32**, 2835–2845 (2012).
19. R. H. Wurtz, W. M. Joiner, R. A. Berman, Neuronal mechanisms for visual stability: Progress and problems. *Philos. Trans. R. Soc. Lond. B Biol. Sci.* **366**, 492–503 (2011).
20. N. Qian, M. E. Goldberg, M. Zhang, Tuning curves vs. population responses, and perceptual consequences of receptive-field remapping. *Front. Comput. Neurosci.* **16**, 1060757 (2023).
21. C. E. Connor, D. C. Preddie, J. L. Gallant, D. C. Van Essen, Spatial attention effects in macaque area V4. *J. Neurosci.* **17**, 3201–3214 (1997).
22. M. Zirnsak, N. A. Steinmetz, B. Noudoost, K. Z. Xu, T. Moore, Visual space is compressed in prefrontal cortex before eye movements. *Nature* **507**, 504 (2014).
23. S. Neupane, D. Guitton, C. C. Pack, Two distinct types of remapping in primate cortical area V4. *Nat. Commun.* **7**, 10402 (2016).
24. A. F. Teich, N. Qian, Learning and adaptation in a recurrent model of V1 orientation selectivity. *J. Neurophysiol.* **89**, 2086–2100 (2003).
25. A. F. Teich, N. Qian, V1 orientation plasticity is explained by broadly tuned feedforward inputs and intracortical sharpening. *Visual Neurosci.* **27**, 57–73 (2010).
26. A. L. Falkner, B. S. Krishna, M. E. Goldberg, Surround suppression sharpens the priority map in the lateral intraparietal area. *J. Neurosci.* **30**, 12787–12797 (2010).
27. J. Schall, D. Hanes, K. Thompson, D. King, Saccade target selection in frontal eye field of macaque. I. Visual and premovement activation. *J. Neurosci.* **15**, 6905–6918 (1995).
28. K. Zhang, Representation of spatial orientation by the intrinsic dynamics of the head-direction cell ensemble: A theory. *J. Neurosci.* **16**, 2112–2126 (1996).
29. C. J. Cueva, A. Ardalan, M. Tsodyks, N. Qian, Recurrent neural network models for working memory of continuous variables: Activity manifolds, connectivity patterns, and dynamic codes. arXiv [Preprint] (2021). https://doi.org/10.48550/arXiv.2111.01275 (Accessed 18 December 2021).
30. L. Matin, D. G. Pearce, Visual perception of direction for stimuli flashed during voluntary saccadic eye movements. *Science* **148**, 1485–1488 (1965).
31. H. Honda, The time courses of visual mislocalization and of extraretinal eye position signals at the time of vertical saccades. *Vision Res.* **31**, 1915–1921 (1991).
32. J. Schlag, M. Schlag-Rey, Through the eye, slowly; Delays and localization errors in the visual system. *Nat. Rev. Neurosci.* **3**, 191–191 (2002).
33. J. Ross, M. C. Morrone, D. C. Burr, Compression of visual space before saccades. *Nature* **386**, 598 (1997).
34. M. Lappe, H. Awater, B. Krekelberg, Postsaccadic visual references generate presaccadic compression of space. *Nature* **403**, 892–895 (2000).
35. C. E. Connor, J. L. Gallant, D. C. Preddie, D. C. Van Essen, Responses in area V4 depend on the spatial relationship between stimulus and attention. *J. Neurophysiol.* **75**, 1306–1308 (1996).
36. N. Qian, "Receptive-field remapping and space representation across saccades" in *Asian Pacific Conference on Vision* (Singapore, 2024), 10-12 July 2024. https://www.apcv2024.com/program. Accessed 30 June 2024.
37. X. Wang, S. Tsien, M. E. Goldberg, M. Zhang, N. Qian, A circuit model for transsaccadic space updating and mislocalization. bioRxiv [Preprint] (2024). https://doi.org/10.1101/2024.10.27.620527 (Accessed 28 October 2024).
38. N. Qian, T. J. Sejnowski, "Learning to solve random-dot stereograms of dense and transparent surfaces with recurrent backpropagation" in *Proceedings of the 1988 Connectionist Models Summer School*, (Morgan Kaufmann, San Mateo, CA, 1989), pp. 435–443.
39. J. W. Bisley, B. S. Krishna, M. E. Goldberg, A rapid and precise on-response in posterior parietal cortex. *J. Neurosci.* **24**, 1833–1838 (2004).
40. M. A. Sommer, R. H. Wurtz, A pathway in primate brain for internal monitoring of movements. *Science* **296**, 1480–1482 (2002).
41. B. Y. Xu, C. Karachi, M. E. Goldberg, The postsaccadic unreliability of gain fields renders it unlikely that the motor system can use them to calculate target position in space. *Neuron* **76**, 1201–1209 (2012).
42. P. Seriès, A. A. Stocker, E. P. Simoncelli, Is the homunculus "aware" of sensory adaptation? *Neural Comput.* **21**, 3271–3304 (2009).
43. H. Xu, P. Dayan, R. M. Lipkin, N. Qian, Adaptation across the cortical hierarchy: Low-level curve adaptation affects high-level facial-expression judgments. *J. Neurosci.* **28**, 3374–3383 (2008).
44. H. Xu, P. Liu, P. Dayan, N. Qian, Multi-level visual adaptation: Dissociating curvature and facial-expression aftereffects produced by the same adapting stimuli. *Vision Res.* **72**, 42–53 (2012).
45. C. D. Gilbert, Adult cortical dynamics. *Physiol. Rev.* **78**, 467–485 (1998).
46. Y.-X. Fu, Y. Shen, H. Gao, Y. Dan, Asymmetry in visual cortical circuits underlying motion-induced perceptual mislocalization. *J. Neurosci.* **24**, 2165–2171 (2004).
47. S. Ding, C. J. Cueva, M. Tsodyks, N. Qian, Visual perception as retrospective Bayesian decoding from high- to low-level features. *Proc. Natl. Acad. Sci. U.S.A.* **114**, E9115–E9124 (2017), 10.1073/pnas.1706906114.
48. L. Luu, M. Zhang, M. Tsodyks, N. Qian, Cross-fixation interactions of orientations suggest high-to-low-level decoding in visual working memory. *Vision Res.* **190**, 107963 (2022).
49. T. Teichert, S. Klingenhoefer, T. Wachtler, F. Bremmer, Perisaccadic mislocalization as optimal percept. *J. Vision* **10**, 19 (2010).
50. N. Qian, R. A. Andersen, A physiological model for motion-stereo integration and a unified explanation of Pulfrich-like phenomena. *Vision Res.* **37**, 1683–1698 (1997).
51. X. Wang, M. Zhang, I. S. Cohen, M. E. Goldberg, The proprioceptive representation of eye position in monkey primary somatosensory cortex. *Nat. Neurosci.* **10**, 640–646 (2007).
52. Y. Xu, X. Wang, C. Peck, M. E. Goldberg, The time course of the tonic oculomotor proprioceptive signal in area 3a of somatosensory cortex. *J. Neurophysiol.* **106**, 71–77 (2011).
53. J. Pola, Models of the mechanism underlying perceived location of a perisaccadic flash. *Vision Res.* **44**, 2799–2813 (2004).
54. Y.-E. Berreby, S. Krishna, How forward remapping predicts perisaccadic biphasic mislocalization. OSF [Preprints] (2025). https://doi.org/10.31219/osf.io/bkaep_v2 (Accessed 2 April 2025).
55. D. C. Burr, M. C. Morrone, Constructing stable spatial maps of the word. *Perception* **41**, 1355–1372 (2012).
56. D. C. Burr, M. C. Morrone, Vision: Keeping the world still when the eyes move. *Curr. Biol.* **20**, R442–R444 (2010).
57. D. C. Burr, M. C. Morrone, Spatiotopic coding and remapping in humans. *Philos. Trans. R. Soc. Lond. B Biol. Sci.* **366**, 504–515 (2011).
58. G. M. Cicchini, P. Binda, D. C. Burr, M. C. Morrone, Transient spatiotopic integration across saccadic eye movements mediates visual stability. *J. Neurophysiol.* **109**, 1117–1125 (2013).
59. S. M. Jeffries, M. Kusunoki, J. W. Bisley, I. S. Cohen, M. E. Goldberg, Rhesus monkeys mislocalize saccade targets flashed for 100 ms around the time of a saccade. *Vision Res.* **47**, 1924–1934 (2007).
60. G. Weng, A. Akbarian, K. Clark, B. Noudoost, N. Nategh, Neural correlates of perisaccadic visual mislocalization in extrastriate cortex. *Nat. Commun.* **15**, 6335 (2024).
61. X. Meng, N. Qian, The oblique effect depends on perceived, rather than physical, orientation and direction. *Vision Res.* **45**, 3402–3413 (2005).
62. S. Suzuki, P. Cavanagh, Focused attention distorts visual space: An attentional repulsion effect. *J. Exp. Psychol. Hum. Percept. Perform.* **23**, 443 (1997).
63. J. Pratt, N. B. Turk-Browne, The attentional repulsion effect in perception and action. *Exp Brain Res.* **152**, 376–382 (2003).
64. K. Anton-Erxleben, C. Henrich, S. Treue, Attention changes perceived size of moving visual patterns. *J. Vision* **7**, 5.1–5.9 (2007).
65. F. Ostendorf, C. Fischer, B. Gaymard, C. Ploner, Perisaccadic mislocalization without saccadic eye movements. *Neuroscience* **137**, 737–745 (2006).
66. W. M. Shim, P. Cavanagh, Bi-directional illusory position shifts toward the end point of apparent motion. *Vision Res.* **46**, 3214–3222 (2006).
67. K. Watanabe, K. Yokoi, Object-based anisotropies in the flash-lag effect. *Psychol. Sci.* **17**, 728–735 (2006).
68. E. Brenner, R. J. van Beers, G. Rotman, J. B. Smeets, The role of uncertainty in the systematic spatial mislocalization of moving objects. *J. Exp. Psychol. Hum. Percept. Perform.* **32**, 811 (2006).
69. X. Wang *et al*., Data from "A circuit model for transsaccadic space updating and mislocalization." Mendeley. https://dx.doi.org/10.17632/2p5vhm2w8n.1. Deposited 16 March 2025.
70. X. Wang *et al*., Data from "Perisaccadic and attentional remapping of receptive fields in lateral intraparietal area and frontal eye fields." Mendeley. https://dx.doi.org/10.17632/w6y53574zp.1. Deposited 18 February 2024.